

# Independent core propagation in two-core photonic crystal fibers resulting from structural nonuniformities

Kristen Lantz Reichenbach and Chris Xu

School of Applied and Engineering Physics, Cornell University, Ithaca, NY 14853  
[KPL22@cornell.edu](mailto:KPL22@cornell.edu)

**Abstract:** Random nonuniformities in the photonic crystal lattice are shown to reduce the coupling length and the coupling efficiency of two-core photonic crystal fibers. These coupling properties are extremely sensitive to imperfections when the air holes are large; variations in the lattice of less than 1% are sufficient to cause essentially independent core propagation due to a drastic reduction in the efficiency of the core coupling. The observed sensitivity of two-core fibers to lattice imperfections is explained through a comparison with coupled mode theory.

© 2005 Optical Society of America

**OCIS Codes:** (060.2400) Fiber properties; (060.2280) Fiber design and fabrication

---

## References and links

1. K. Saitoh, Y. Sato and M. Koshiba, "Coupling characteristics of dual-core photonic crystal fiber couplers," *Opt. Express* **11**, 3188-3195 (2003). <http://www.opticsexpress.org/abstract.cfm?URI=OPEX-11-24-3188>.
2. L. Zhang and C. Yang, "Polarization splitter based on photonic crystal fibers," *Opt. Express* **11**, 1015-1020 (2003). <http://www.opticsexpress.org/abstract.cfm?URI=OPEX-11-9-1015>.
3. D. Chremmos, G. Kakarantzas and N. K. Uzunoglu, "Modeling of a highly nonlinear chalcogenide dual-core photonic crystal fiber coupler," *Opt. Commun.* **251**, 339-345 (2005).
4. K. L. Reichenbach and C. Xu, "The effects of randomly occurring nonuniformities on propagation in photonic crystal fibers," *Opt. Express* **13**, 2799-2807 (2005). <http://www.opticsexpress.org/abstract.cfm?URI=OPEX-13-8-2799>.
5. T. P. White, B. T. Kuhlmeiy, R. C. McPhedran, D. Maystre, G. Renversez, C. M. d. Sterke and L. C. Botten, "Multipole method for microstructured optical fibers. I. Formulation," *J. Opt. Soc. Am. B* **19**, 2322-2330 (2002).
6. B. T. Kuhlmeiy, T. P. White, G. Renversez, D. Maystre, L. C. Botten, C. M. d. Sterke and R. C. McPhedran, "Multipole method for microstructured optical fibers. II. Implementation and results," *J. Opt. Soc. Am. B* **19**, 2331-2340 (2002).
7. CUDOS MOF UTILITIES Software ©Commonwealth of Australia 2004. All rights reserved. <http://www.physics.usyd.edu.au/cudos/mofsoftware/>.
8. A. Snyder and J. Love, *Optical Waveguide Theory* (Kluwer, London, 1983).
9. C. Vassallo, *Optical Waveguide Concepts* (Elsevier, Amsterdam, 1991).
10. A. Barybin and V. Dmitriev, *Modern Electrodynamics and Coupled-Mode Theory: Application to Guided-Wave Optics* (Rinton Press, 2002).
11. S. L. Chuang, *Physics of Optoelectronic Devices* (Wiley-Interscience, 1995).

---

## 1. Introduction

The design flexibility and unique propagation characteristics of photonic crystal fibers (PCFs) offer many new possibilities for fiber based devices. Multiple core PCFs with novel air hole arrangements take advantage of these properties for applications such as filters, couplers, switches, and polarization splitters [1-3]. The realization and performance of these designs depend on the predictability of the coupling behavior between cores. Accurate numerical methods exist for simulating multi-core PCFs and their properties; however, fabrication processes generate random nonuniformities in the photonic crystal lattice that can potentially alter the actual performance of the fiber from that which is predicted by simulation. By

imposing random variations in the air hole size and in the air hole location of two-core PCFs and then using numerical simulation tools to calculate certain properties of these fibers, a better understanding of the impact of fabrication induced irregularities can be gained.

The rate and the efficiency of power transfer between cores are important parameters to examine when designing a fiber coupler or any other device that utilizes the properties of a multi-core fiber. Previous work has shown that the rate of power transfer between the cores of two-core photonic crystal fibers, described by the coupling length, can be extremely sensitive to irregularities in the “cladding” of the PCF, or the lattice surrounding the cores [4]. For large air hole fibers, nonuniformities in the photonic crystal lattice of less than 1% were shown to produce, on average, a deviation in the coupling length of at least an order of magnitude from the predicted value which is calculated from a fiber with a perfect lattice [4]. In this paper, we demonstrate numerically that in addition to decreasing the coupling length, imperfections in the photonic crystal lattice drastically reduce the coupling efficiency, or the fraction of the power that is transferred between cores, depending on the relative size of the air holes. Two-core fibers with relatively small air holes and shorter coupling lengths are markedly more robust to nonuniformities than two-core PCFs with large air holes and long coupling lengths. The coupling efficiency is shown to be minimal for fibers with large air holes when only small nonuniformities are present, resulting in essentially independent core propagation. The effects of imperfections in the lattice on the coupling properties of two-core PCFs, as well as the dependence of this response on the size of the air holes, are explained through a comparison with coupled mode theory.

An obvious approach to achieving independent core propagation in a multi-core fiber is to engineer a long coupling length by increasing the core separation and the mode confinement. This method, however, places restrictions on the fiber design as well as how densely the cores can be packed in a fiber. An alternative solution is to decrease the efficiency of the coupling such that an insignificant amount of power is transferred between the cores regardless of the coupling length or the rate of the coupling. Our results show that structural nonuniformities in two-core PCFs that could be a consequence of normal fabrication processes have the potential to drastically reduce the efficiency of the coupling allowing coupling to be practically ignored. The imperfections in the cladding cause the two cores to become decoupled and, as a result, light propagates essentially independently in each core.

## 2. Method

In order to understand how the introduction of nonuniformities affects the core coupling in a two-core PCF, we use a vector normal mode expansion to compare how power in each core fluctuates as a function of the propagation distance for many randomly generated fibers with imperfect lattice structures and for fibers without imperfections.

The PCFs simulated are composed, in cross-section, of air holes arranged in a triangular lattice around two silica defects separated by a single air hole, as shown in Figs. 1(a) and 1(b). The  $x$  and  $y$  axes are also defined in 1(a). The guided field in the waveguide,  $\vec{E}(x, y, z)$  and  $\vec{H}(x, y, z)$ , is expressed as an expansion of the bound modes of a particular two-core PCF following Eq. (1) [8, 9]:

$$\vec{E}(x, y, z) = \sum_j a_j \vec{e}_j(x, y) \exp(i\beta_j z), \quad (1)$$

likewise for  $\vec{H}(x, y, z)$ , where  $\beta_j$  is the propagation constant or eigenvalue of the  $j^{\text{th}}$  mode,  $\vec{e}_j(x, y)$  is the modal field, and the  $z$ -direction is parallel to the axis of the fiber. The modal amplitudes,  $a_j$ , represent the amount of overlap between the input field and the  $j^{\text{th}}$  mode and

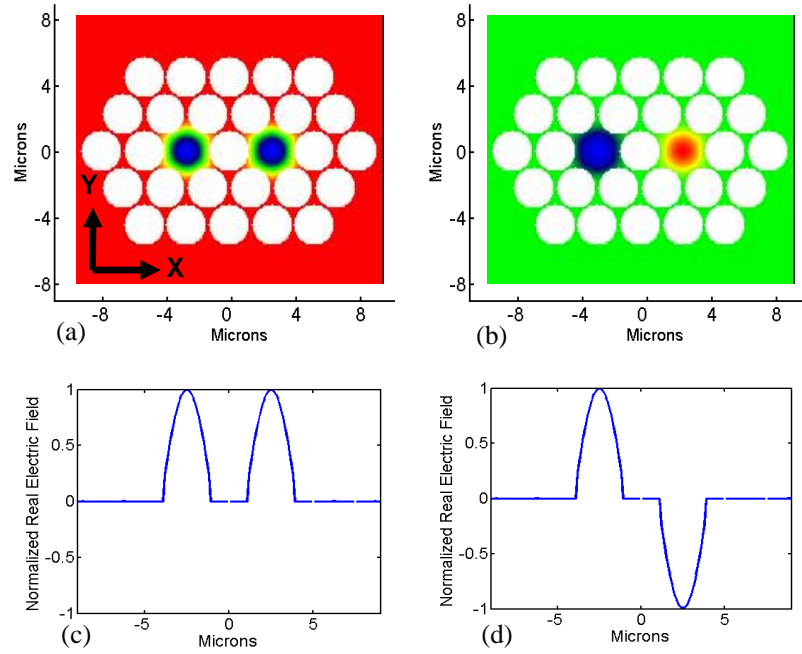


Fig. 1. The x-polarized modes ( $E_x$  is much larger than  $E_y$ ) of the fundamental mode group for a perfect lattice two-core PCF with  $d/\Lambda=0.90$  and  $\Lambda=2.5\mu\text{m}$ . (a) and (b) display the PCF cross-section and the real x-component of the electric field; the white circles are air holes. (c) and (d) show the profile of the field along  $y=0$ ; (a) and (c) are a symmetric mode, while (b) and (d) are antisymmetric.

are determined from Eq. (2) [8, 9]:

$$a_j = \frac{1}{2N_j} \iint_{\infty} \vec{E}(x, y, 0) \times \vec{h}_j^*(x, y) \cdot \hat{z} dx dy, \quad (2)$$

where  $\vec{E}(x, y, 0)$  is the input field and  $\vec{h}_j(x, y)$  is the modal magnetic field.  $N_j$  determines the normalization of the  $j^{\text{th}}$  mode as defined in Eq. (3):

$$\frac{1}{2} \iint_{\infty} \vec{e}_j(x, y) \times \vec{h}_j^*(x, y) \cdot \hat{z} dx dy = \frac{1}{2} \iint_{\infty} \vec{e}_j^*(x, y) \times \vec{h}_j(x, y) \cdot \hat{z} dx dy = N_j \quad (3)$$

The power as a function of  $z$  in a particular core is calculated from the Poynting vector using Eq. (4):

$$P_{\text{core}}(z) = \frac{1}{2} \text{Re} \iint_{\text{core area}} \vec{E}(x, y, z) \times \vec{H}^*(x, y, z) \cdot \hat{z} dx dy, \quad (4)$$

where the guided fields are calculated following Eq. (1) and the core area is assigned as the area on either side of a line that bisects the central air hole along  $x=0$ . The coupling efficiency, or the percentage of power transferred between cores, as well as the rate of power transfer, or the coupling length, are determined from Eq. (4). The input field is x-polarized,

$E_y=0$ , and has a Gaussian profile that is centered on the left core with a spot diameter ( $1/e^2$  intensity) equal to the pitch. Reflections at the input interface are ignored.

The photonic crystal lattice that makes up the cladding of a PCF is described by two parameters: the air hole diameter,  $d$ , and the air hole separation or pitch,  $\Lambda$ . Nonuniformities are introduced into the fiber by independently imposing stochastic variations on the air hole size and on the location of the air holes in the same manner as Ref. [4]. Each imperfect two-core PCF is generated by randomly assigning every air hole in the fiber a value from a Gaussian distribution of values for  $d$  or  $\Lambda$ . The degree of irregularity in the lattice is defined as the ratio of the standard deviation to the mean of this distribution (ie.  $\delta d/d_0$  or  $\delta\Lambda/\Lambda_0$ ) times 100, or as a percentage of variation. The average value used for the pitch is always  $2.5\mu\text{m}$ , unless otherwise stated, therefore a variation of 1% indicates that the standard deviation of the imposed structural perturbations is 25nm. The modal fields and the mode propagation constants of two-core PCF structures with and without imperfections are calculated for the wavelength of light of  $1.55\mu\text{m}$  using numerical simulations based on the multipole method [5-7]. The highest index mode group contains four modes with slightly different indices whose energy distributions within the individual cores are all approximately Gaussian with azimuthal symmetry, as characteristic of a fundamental mode. The normal mode expansion is truncated after these four lowest order modes since they represent the most significant contribution to the sum due to their large overlap with the input field. Our modeling showed that ignoring the higher order modes results in negligible error because the modal amplitudes,  $a_j$ , are extremely small.

### 3. Results

The power in the left and right cores as a function of  $z$  is shown in Fig. 2 for a two-core PCF with  $d/\Lambda=0.58$ . Figure 2(a) shows the power transfer when the lattice of the fiber is perfectly uniform. Because the two cores are identical, energy is distributed equally between the cores for each of the four modes in the fundamental mode group. The two highest index modes in this group exhibit symmetric behavior when the amplitude of the field is considered, while the lowest two are antisymmetric. The symmetric and antisymmetric modes that are predominantly x-polarized are displayed in Fig. 1. Polarized light incident on one of the cores is represented by a linear superposition of a symmetric and an antisymmetric eigenmode of the two-core system, each of which propagate according to a slightly different effective propagation constant. The beating of the eigenmodes causes power to oscillate between cores as a function of the propagation distance along the fiber. Figure 2(a) shows that, as expected, after a propagation distance equal to the coupling length,  $\sim 2000\mu\text{m}$ , one hundred percent of the power transfers from one core to the other because the energy is equally distributed between the cores for the eigenmodes of the structure. Introducing a random variation of

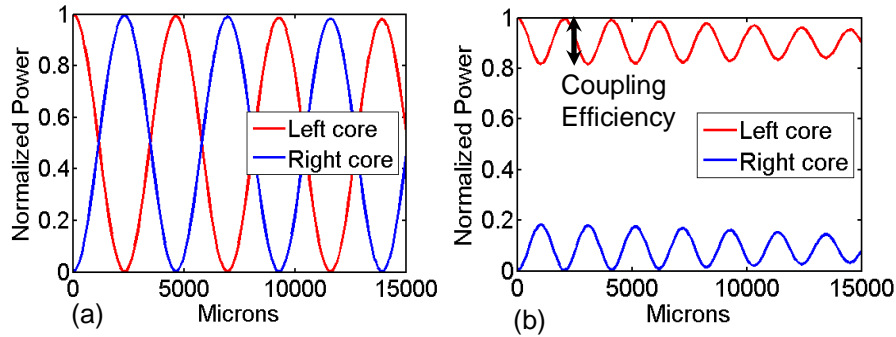


Fig. 2. The normalized power in each core is plotted versus the propagation distance. The coupling efficiency changes from (a) 1 to (b) 0.20 when a random variation of 2.2% in the air hole size is introduced,  $\Lambda = 2.5 \mu\text{m}$  and  $d/\Lambda = 0.58$ .

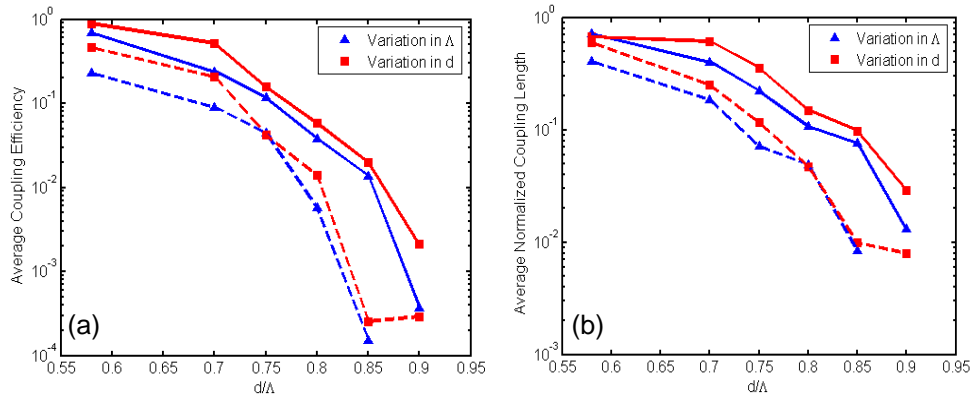


Fig. 3. The average coupling efficiency (a) and the average coupling length, normalized to the value for a perfectly uniform structure, (b) are plotted vs.  $d/\Lambda$  for a percentage variation of 1% (solid line) and 4% (dashed line),  $\Lambda = 2.5 \mu\text{m}$ . The lines have been added to facilitate the eye.

2.2% in the air hole size caused, in this particular structure, the coupling length to be reduced by half and the efficiency of the coupling to decrease to 20% as shown in Fig. 2(b). The definition of the coupling efficiency as it is referred to elsewhere in this paper is illustrated in Fig. 2(b).

In Fig. 3(a), the coupling efficiency is plotted versus the relative air hole size,  $d/\Lambda$ , for two different values of the percentage variation for each type of variation. Each marker represents the average efficiency of a data set containing thirty randomly generated two-core PCFs. As the relative size of the air holes increases, and as the nonuniformity in the fiber increases, the coupling efficiency decreases. Large air hole two-core fibers exhibit extremely low coupling efficiency; for example, a PCF with  $d/\Lambda=0.90$  and structural imperfections of only 1% will have a coupling efficiency, on average, of less than 1%.

The coupling length exhibits a similar response to lattice variations, as shown in Fig. 3(b), where the average normalized coupling length is plotted versus  $d/\Lambda$ . In order to examine the relationship between these two properties of two-core PCFs, the coupling efficiency is plotted versus the coupling length in Fig. 4 for different values of  $d/\Lambda$ . Each marker represents the coupling efficiency and the coupling length of a randomly generated two-core fiber with variations of 0.67% to ~4% in either the air hole size or the air hole separation. Fibers with large air holes (bottom right) typically exhibit a coupling efficiency of less than 1%.

All the structures examined in Fig. 4 are multi-moded. By increasing the wavelength to pitch ratio (i.e. the normalized wavelength) for the relative air hole sizes studied here, or by decreasing the value of  $d/\Lambda$  into the endlessly single mode regime, a single mode will be guided. Changing the structure by increasing the normalized wavelength results in a larger mode size as does decreasing the air hole size; therefore, altering the normalized wavelength in this manner should follow the same trend shown in Fig. 4 for changes in  $d/\Lambda$ . This is indeed the case. Data in Fig. 4 moves up and to the left as the structure becomes less multi-moded because of changes in the air hole size or in the normalized wavelength. This behavior demonstrates that two-core fibers become less sensitive to variations as the coupling length decreases and the mode field area becomes larger.

Upon inspection of the plots in Fig. 4, the efficiency is noticed to decrease at a quicker rate than the coupling length in a clear power relationship, inferred from the linear distribution of data points in the log-log plots. The fact that the data exhibits similar slopes across all plots indicates that the nature of the relationship between these parameters does not appear to depend on the relative air hole size. A linear fit of the log-log data reveals an approximately quadratic relationship between the two parameters, as evidenced by the slope values given in Table 1 shown for each of the plots in Fig. 4. In order to develop an understanding of this relationship, we applied coupled mode theory to two-core PCFs with imperfect lattice structures.

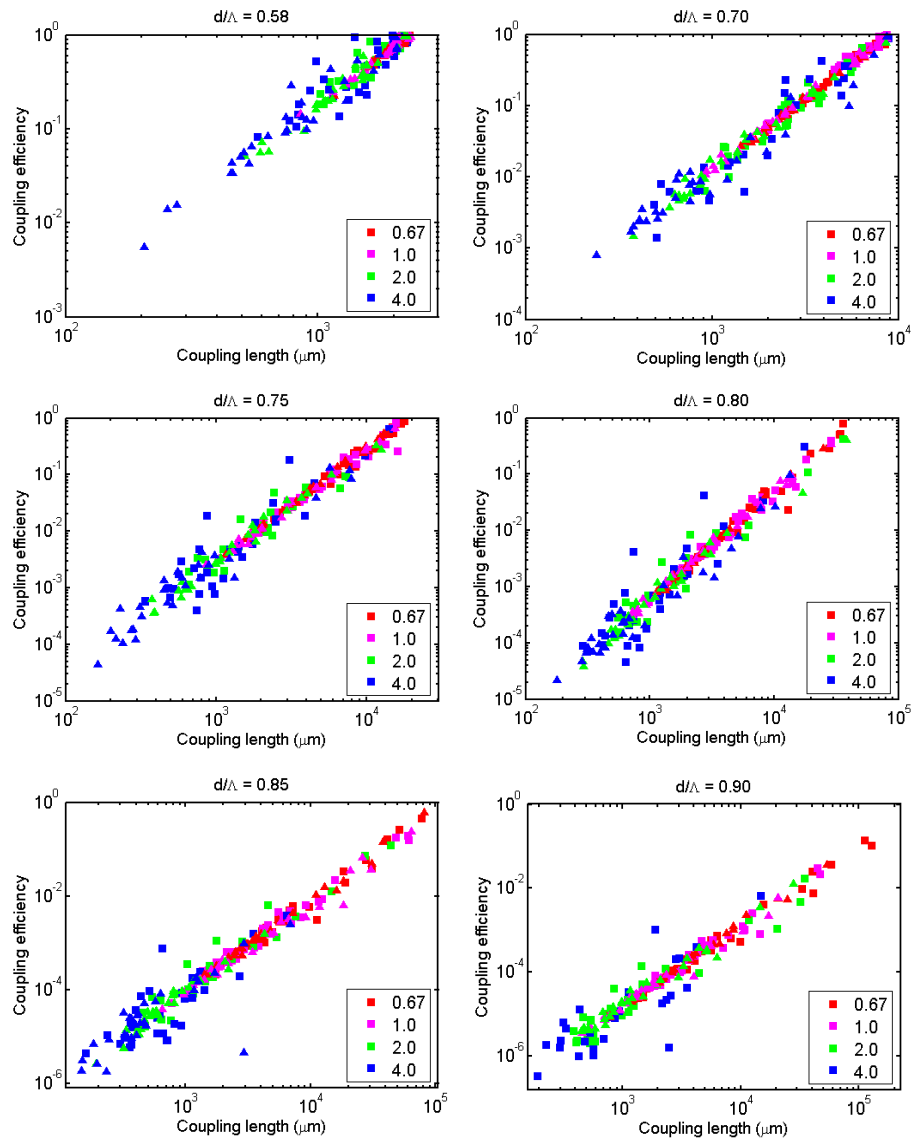


Fig. 4. The coupling efficiency vs. the x polarization coupling length for  $\Lambda = 2.5$   $\mu\text{m}$  and  $d/\Lambda = 0.58, 0.70, 0.75, 0.80, 0.85$  and  $0.90$  from upper left to lower right. Note that the axis scaling differs for each plot.

Table 1. The slopes of linear fits to the log-log data of Fig. 4.

d/Λ	Slope
0.58	1.93
0.70	1.94
0.75	1.93
0.80	1.88
0.85	1.92
0.90	1.91

#### 4. Couple mode theory

In coupled mode theory (CMT), each core is treated as an independent waveguide that is perturbed by the presence of fields propagating in the other core. When the field from one core enters the high index core region of the second waveguide, it becomes a source for a new field. The total field solution of a system of two waveguides, label them  $a$  and  $b$ , is approximated as a linear combination of the mode fields of the individual waveguides [11], as shown in Eq. (5).

$$\begin{aligned}\vec{E}(x, y, z) &= a(z)\vec{e}^a(x, y) + b(z)\vec{e}^b(x, y) \\ \vec{H}(x, y, z) &= a(z)\vec{h}^a(x, y) + b(z)\vec{h}^b(x, y)\end{aligned}\quad (5)$$

In the weak coupling regime, the cross power (proportionally to the area integrals of  $\vec{e}_t^a(x, y) \times \vec{h}_t^b(x, y)$  and  $\vec{e}_t^b(x, y) \times \vec{h}_t^a(x, y)$ ) is ignored and the amplitudes of the two cores obey the coupled amplitude equations of Eq. (6) as derived from the general reciprocity relation [11].

$$\begin{aligned}\frac{d}{dz}a(z) &= i\beta_a a(z) + iK_{ab}b(z) \\ \frac{d}{dz}b(z) &= iK_{ba}a(z) + i\beta_b b(z)\end{aligned}, \quad (6)$$

where  $\beta_a$  and  $\beta_b$  are the propagation constants for the individual, independent waveguides and the coupling coefficients,  $K_{ba}$  and  $K_{ab}$ , are proportional to the overlap integral of the mode fields of the individual waveguides in each core [10, 11]. Solving this system of equations and applying the initial condition that light is incident on waveguide  $a$  at  $z = 0$ , or  $a(0) = 1$  and  $b(0) = 0$ , produces the expression for the power in waveguide  $b$  given in Eq. (7) [11]:

$$\begin{aligned}P_b(z) &= |b(z)|^2 = \left| \frac{K_{ab}}{\psi} \right|^2 \sin^2 \psi z, \\ \text{where : } \psi &= \sqrt{\frac{(\beta_b - \beta_a)^2}{4} + K_{ab}K_{ba}},\end{aligned}\quad (7)$$

The coupling properties of the two-core PCF are again defined from the power transfer,  $P_b(z)$ . The coupling length is the distance,  $L_c$ , at which the power in waveguide  $b$  has oscillated to its first maximum, ie.  $\psi L_c = \pi/2$ . The coupling efficiency can be defined from Eq. (7) as the maximum possible value for the power in waveguide  $b$ , or  $|K_{ab}/\psi|^2$ . As the mismatch between the modes,  $\beta_b - \beta_a$ , increases, it can be seen from these relationships that the coupling efficiency and the coupling length will decrease. When the variable  $\psi$  is solved for in the expression for the coupling length and substituted into the expression for the coupling efficiency, the efficiency is shown to be proportional to the square of the coupling length:

$$Efficiency = \frac{4|K_{ab}|^2}{\pi^2} L_c^2 \quad (8)$$

Improved coupled mode theory, where the coupling is no longer assumed to be weak, results in the same relationship between the efficiency and the coupling length as in Eq. (8), but with a different proportionality constant still dependent on the mode overlap that is modified by an amount determined by the cross power [10, 11]. For simplicity, we will continue without including the effects of the cross power. The quadratic relationship of Eq. (8) substantiates the relationship predicted from the power law fits of the plots in Fig. 4 and from the values in Table 1.

The applicability of CMT can be further assessed by comparing the coupling length,  $L_c$ , as calculated from CMT using Eq. (8) to the value derived directly through the multipole method for a perfect structure. Beginning with Eq. (8), if  $K_{ab}$  is assumed to be constant, a quadratic polynomial fit, where the linear and zeroth order terms in the polynomial are forced to be zero, can be applied to the data of Fig. 4 and the fit parameter can be used to estimate  $K_{ab}$ . The assumption that  $K_{ab}$  is constant claims that the induced structural perturbations do not significantly change the amount of overlap between the mode fields of the two cores from that of a uniform two-core PCF. Table 2 lists the fit parameters from the quadratic fit for each ratio of  $d/\Lambda$  studied and the coupling coefficient,  $K_{ab}$ , as solved for from these values. An estimate of the coupling length for a perfect fiber can be calculated from  $K_{ab}$  using CMT and Eq. (7) with a mismatch set to zero. These values are compared in the final two columns of Table 2 with the coupling length as determined directly from two-core fibers with a perfectly uniform photonic crystal lattice. This comparison implies that CMT in the weak coupling regime adequately describes the behavior of these two-core PCFs when nonuniformities are

Table 2. The fit parameter, or the coefficient of a quadratic fit to the data in Fig. 4, is listed according to the relative air hole size.  $K_{ab}$  is calculated from the fit parameter according to Eq. (8). The final columns compare the coupling length as calculated from the fit using CMT with the value determined directly from the perfect structure.

$d/\Lambda$	Fit parameter ( $\mu\text{m}^{-2}$ )	$ K_{ab} $ ( $\mu\text{m}^{-1}$ )	CMT $L_c$ ( $\mu\text{m}$ )	$L_c$ ( $\mu\text{m}$ )
0.58	1.88E-07	6.82E-04	2.30E+03	2.32E+03
0.70	1.23E-08	1.74E-04	9.01E+03	8.89E+03
0.75	2.74E-09	8.22E-05	1.91E+04	1.83E+04
0.80	4.25E-10	3.24E-05	4.85E+04	4.16E+04
0.85	7.41E-11	1.35E-05	1.16E+05	1.03E+05
0.90	8.66E-12	4.62E-06	3.40E+05	2.49E+05

present. The discrepancy between the values for  $L_c$  from the two methods most likely results from neglecting the cross power and from the parameter  $K_{ab}$  not remaining constant for all imperfect structures. In fact, for a few cases, generated imperfect two-core PCFs exhibited longer coupling lengths than a fiber with a perfectly uniform lattice; in order to satisfy Eq. (8) without predicting an efficiency greater than one,  $K_{ab}$  would have to be much different than that of the perfect fiber. The data from these structures was left out of the fit on the basis that it did not satisfy the condition that  $K_{ab}$  be approximately constant. Revisiting the power law fit results shown in Table 1 with these data points removed leads to fits that are closer to quadratic; for example, for  $d/\Lambda=0.58$  and  $d/\Lambda=0.70$ , the slopes increase to 1.98 and 1.99 respectively.

## 5. Discussion

Nonuniformities in the lattice structure of two-core PCFs cause the cores to be no longer identical, thus creating a mismatch in the indices of the fundamental modes of the two individual cores. A nonzero mismatch results in a decreased coupling length and coupling efficiency as compared with the values that would be predicted from a perfect structure with no mismatch. The coupling properties of a two-core fiber structure with imperfections are determined by the parameter  $\psi$ , as defined in Eq. (7), which depends on both the mismatch and  $K_{ab}$ . Thus, knowledge of  $K_{ab}$  alone, which can be gained from simulations based on a perfect two-core fiber, is not sufficient to accurately predict the coupling behavior of a particular PCF that is not completely uniform. It is the magnitude of the mismatch relative to  $K_{ab}$  that determines how different the core coupling will be from that of a perfect structure. If  $K_{ab}$  is small relative to the induced mismatch, the fiber is more sensitive and the coupling properties will change significantly when nonuniformities—and therefore core mismatch—are introduced. For example,  $K_{ab}$ , which is proportional to the mode overlap, will be smaller when the modes are well confined, which is generally true of PCFs with large air holes (see Table 2). The magnitude of the mismatch, or  $\beta_b - \beta_a$ , can be estimated from the birefringence induced in a single core PCF when nonuniformities are introduced into the cladding structure. From Ref. [4], Fig. 2, the average induced birefringence of PCFs with  $d/\Lambda = 0.70$  and  $d/\Lambda = 0.90$  for  $\Lambda=2.5\mu\text{m}$  are shown to be of approximately the same order of magnitude,  $\Delta n \sim 1\text{e-}4$ , across percentage variations of 0.67% to 4%. It can be seen in Table 2 that this  $\Delta n$  is two

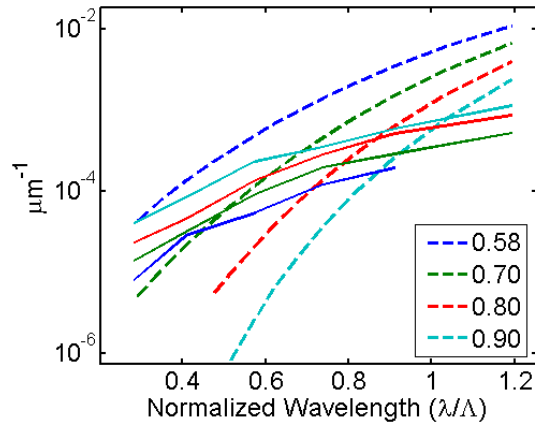


Fig. 5.  $K_{ab}$ , as computed from a perfect structure, (dashed lines) and  $\Delta\beta$ , calculated from the birefringence induced from variations in the lattice of a single core PCF, (solid lines) are plotted versus the normalized wavelength.  $\Delta\beta$  is the average value for 20 structures with variations of 1% in the air hole separation.

orders of magnitude larger than the coupling coefficient,  $K_{ab}$ , for  $d/\Lambda = 0.90$ , while it is actually slightly smaller than  $K_{ab}$  for  $d/\Lambda = 0.70$ . Therefore, the same mode mismatch between two cores will result in a much greater change in the coupling properties when the modes are tightly confined ( $d/\Lambda = 0.90$ ). Clearly, small perturbations have a greater impact on fibers with larger air holes because they are characterized by a relatively large mismatch and a small overlap.

The mismatch and the coupling coefficient do, however, depend on the normalized wavelength. The impact of changing the normalized wavelength on the relative magnitude of these two parameters can be assessed from Fig. 5. The coupling coefficient is calculated from a perfect two-core structure and  $\Delta\beta$  is defined as the mismatch divided by 2 so that the two parameters plotted represent the two contributions to  $\psi$ . The mismatch is calculated in the same manner as in Ref. [4] from the average induced birefringence of a single core PCF with variations in the air hole separation of 1%. Regions of high and low sensitivity to lattice imperfections can be predicted from this plot. When  $\Delta\beta \gg K_{ab}$ , a two-core PCF will generally exhibit high sensitivity to variations; this region corresponds to small  $\lambda/\Lambda$ . On the other hand, when  $\lambda/\Lambda$  is larger,  $K_{ab} \gg \Delta\beta$ , indicating a low sensitivity to structural nonuniformities. In this region, the PCFs tend to have fewer guided modes. Large air hole fibers will, in general, be sensitive to variations over a larger range of wavelengths and it appears that fibers in the single-moded regime, or large  $\lambda/\Lambda$ , are more robust to variations.

Consequences of the non-identical nature of the cores are also manifested through a modification of the mode structure. Exploring the change in the mode shape provides a more intuitive understanding of the impact of nonuniformities on the coupling behavior of two-core PCFs. As stated previously, the eigenmodes of the unperturbed two-core system are perfectly symmetric or antisymmetric in amplitude and distribute energy evenly between the two cores. However, imperfections in the lattice cause the eigenmodes to evolve towards those of the

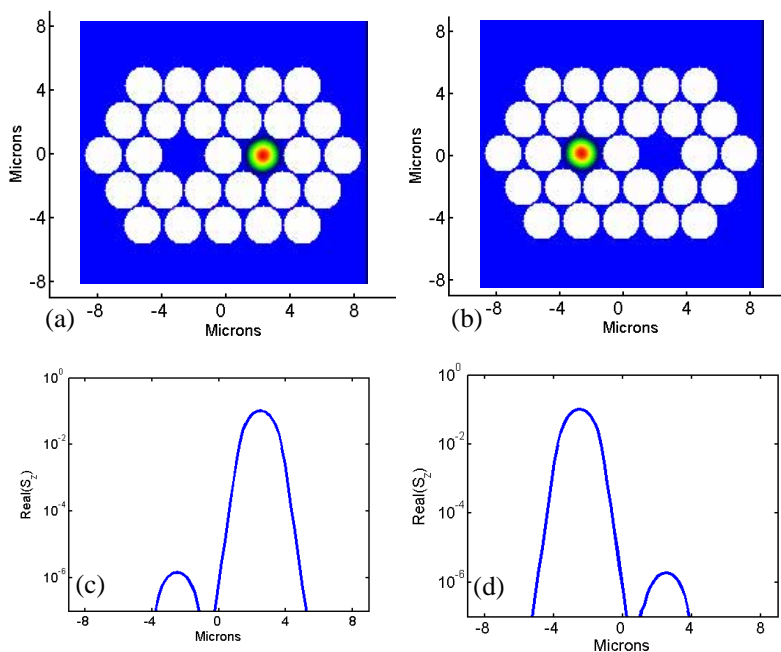


Fig. 6. A cross-sectional view of the z-component of the real part of the Poynting vector for two of the modes from the highest index mode group of a two-core PCF with  $\Lambda = 2.5 \mu\text{m}$  and  $d/\Lambda = 0.90$  and nonuniformities of 0.67% appears in (a) and (b), while (c) and (d) show the profile along the line where  $y = 0$ . Similar behavior is observed for the two other modes in the group.

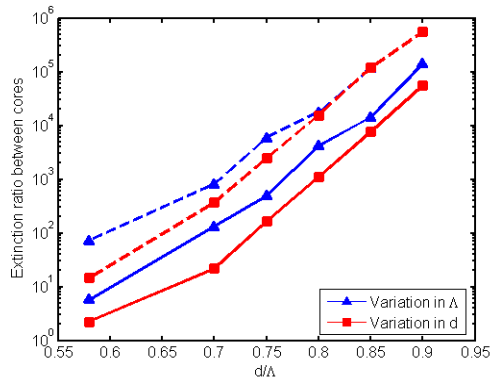


Fig. 7. The ratio of power in the left core to that in the right core for a mode that is predominantly left is shown as a function of the normalized air hole size,  $d/\Lambda$ , for a percentage variation of 1% (solid line) and 4% (dashed line),  $\Lambda = 2.5 \mu\text{m}$ . The lines have been added to facilitate the eye. The value for a perfect two-core fiber is 1.

decoupled cores as evidenced by the z-component of the Poynting vector shown in Fig. 6 for a fiber with  $d/\Lambda=0.90$  and variations of 0.67%. The energy of each mode is almost completely concentrated in one core. Figure 7 shows the extinction ratio between the cores, or the ratio of energy in one core to that in the other, for fibers with different relative air hole sizes and for two degrees of variation in the fiber structure. Each marker is an average over thirty structures. As the percentage of variation in the lattice structure increases, and as the ratio of  $d/\Lambda$  increases, the mode energy becomes more concentrated in one core or the other. When  $d/\Lambda$  is greater than 0.80, the amount of energy localized in one core is, on average, at least three orders of magnitude greater than the energy in the other core for all the fundamental modes of the fiber, even when variations are as small as 1%. The two modes in the fundamental mode group with the highest indices will be almost entirely right (or left) modes while the remaining two modes will be left (or right) modes. From a scalar point of view, this change in the eigenmode structure explains the observed decrease in the coupling efficiency since the single-core input field closely resembles one of the eigenmodes of the perturbed structure. Light that is incident on one of the cores will now couple predominantly into an eigenmode of the system and travel along the fiber according to the propagation constant of this mode with an almost constant transverse energy profile. Large air hole structures are more sensitive to decoupling because the modes are already well confined in the individual cores.

For applications where independent core propagation is a requirement, two opposing approaches exist. A long coupling length achieved by increasing the core separation is the obvious method for obtaining this effect. The results presented in this paper, however, illuminate a more simple solution which is to reduce the coupling efficiency. The cores can be packed very closely but in a photonic crystal lattice that is very sensitive to perturbations, such as a PCF with a high ratio of  $d/\Lambda$  or well confined modes. When even slight nonuniformities are present, the two cores in these PCFs can be assumed to be decoupled and light will propagate independently in each core. Typical variations in the structure due to fabrication can actually drastically reduce the coupling length; however, since the efficiency of the coupling is approximately zero, all coupling can be essentially ignored.

We also note that due to the random nature in which the variations were imposed on the structures simulated in this paper, the results should remain robust to additional perturbations not accounted for, such as bending.

## 6. Conclusion

Through numerically simulating two-core fibers with different air hole sizes and introducing random variations into their cladding structure, we have shown that the coupling length and the coupling efficiency can be altered by imperfections in the photonic crystal lattice and that the sensitivity of these parameters to imperfections depends on the relative air hole size. Two-core PCFs with relatively small air holes or a large normalized wavelength are more robust to nonuniformities where large air hole fibers or fibers with a small normalized wavelength can be extremely sensitive. In fact, for a fiber with  $d/\Lambda=0.90$ ,  $\Lambda=2.5\mu\text{m}$ , and structural variations of only 1%, the average coupling length can be expected to be reduced by two orders of magnitude and the amount of power transferred between the cores will be less than 0.1%. The observed quadratic relationship between the coupling length and the efficiency was confirmed through a comparison with coupled mode theory and the reduced coupling efficiency was explained intuitively by examining the change in the eigenmode shapes. Our results clearly indicate that practically independent core propagation can be easily obtained in a large air hole PCF when structural imperfections are present.

## Acknowledgments

The authors are grateful to John Fini at OFS Optics for insightful discussions about the multipole method and programs based on this method. This research was supported by the National Center for Research Resources (NCR), National Institutes of Health. The authors also acknowledge the University of Sydney through its ARC Centre of Excellence - Ultrahigh-bandwidth Devices for Optical Systems, School of Physics as the exclusive Licensor of the CUDOS MOF UTILITIES Software.